Fatty acid uptake and metabolism in a human intestinal cell line (Caco-2): comparison of apical and basolateral incubation

Pamela J. Trotter and Judith Storch[1]

Department of Nutrition, Harvard School of Public Health and Program in Cell and Developmental Biology, Harvard Medical School, Boston, MA 02115

Abstract Free fatty acids can enter the enterocyte via the apical or basolateral plasma membrane. We have used the Caco-2 intestinal cell line to examine the polarity of free fatty acid uptake and metabolism in the enterocyte. Differentiated Caco-2 cells form polarized monolayers with tight junctions, and express the small intestine-specific enzymes sucrase and alkaline phosphatase. Cells were grown on permeable polycarbonate Transwell filters, thus allowing separate access to the apical and basolateral compartments. Total uptake of [^{3}H]palmitate bound to bovine serum albumin (palmitate-BSA 4:1) was twofold higher ($P < 0.05$ or less) at the apical surface than at the basolateral surface. The relative apical and basolateral membrane surface areas of the Caco-2 cells, as measured by partition of the fluorophore trimethylammonium-diphenylhexatriene (TMA-DPH), was found to be 1:3. Thus, apical fatty acid uptake was sixfold higher than basolateral uptake per unit surface area. Analysis of metabolites after incubation with submicellar concentrations of [^{3}H]palmitate showed that the triacylglycerol to phospholipid (TG:PL) ratio was higher for fatty acid added to the apical as compared to the basolateral compartment (20% at 60 min, $P < 0.025$). Little fatty acid oxidation was observed. Preincubation with albumin-bound palmitate, alone or with monoolein, increased the incorporation of both apical and basolateral free fatty acids into TG. The results suggest that the net uptake of long-chain free fatty acids across the apical plasma membrane is greater than uptake across the basolateral membrane. In addition, a small increase in the TG:PL ratio for apically, compared to basolaterally, added free fatty acids suggests that polarity of metabolism occurs to a limited extent in Caco-2 enterocytes.—**Trotter, P. J., and J. Storch.** Fatty acid uptake and metabolism in a human intestinal cell line (Caco-2): comparison of apical and basolateral incubation. *J. Lipid Res.* 1991. **32:** 293-304.

Supplementary key words enterocytes • cell polarity • membrane surface area • trimethylammonium-diphenylhexatriene

Long chain free fatty acids (FFA) are major hydrolysis products of dietary fat in the lumen of the intestine, and are subsequently absorbed by the enterocytes that line the small intestine. After uptake across the microvillus (apical) plasma membrane, FFA are reincorporated into triacylglycerol (TG) and phospholipid (PL), packaged into lipoprotein particles, and secreted into the lymph via the serosal (basolateral) membrane (1, 2).

FFA from the plasma are also taken up into the enterocyte via the basolateral membrane. Plasma FFA have been reported to be metabolized differently than those absorbed from the lumen. In 1975, Gangl and Ockner (3) reported that when rats were administered FFA by duodenal infusion or via intravenous injection and metabolism by the small intestinal epithelium was analyzed, FFA absorbed from the lumen were mainly incorporated into TG, whereas FFA taken up from the plasma were primarily oxidized or incorporated into PL. A similar study using human jejunal biopsy samples also showed that plasma FFA were preferentially incorporated into PL or oxidized (4). Similar metabolic polarity was evident in both villus and crypt cells (3). The observed polarity of FFA metabolism in the intestinal epithelium was thought to be at the level of the enterocyte (3); however FFA metabolic polarity at the cellular level has not yet been directly demonstrated.

The mechanism of FFA uptake across the enterocyte plasma membrane is also not definitively understood. Although long thought to occur by passive diffusion (5, 6), long chain FFA uptake into the enterocyte has recently been proposed to occur via a specific and saturable pro-

Abbreviations: BSA, bovine serum albumin; CE, cholesteryl ester; DG, diacylglycerol; FABP, fatty acid-binding protein; $FABP_{PM}$, plasma membrane fatty acid-binding protein; FFA, free fatty acids; I-FABP, intestinal FABP; L-FABP, liver FABP; MG, monoacylglycerol; PA, phosphatidic acid; PBS, phosphate-buffered saline; PBS-GCM, PBS supplemented with glucose, $CaCl_2$, and $MgCl_2$; PC, phosphatidylcholine; PE, phosphatidylethanolamine; PL, phospholipid; PS, phosphatidylserine; TG, triacylglycerol; TMA-DPH, 1-[4-(trimethylamino)-phenyl]-6-phenylhexatriene; TLC, thin-layer chromatography.

[1]To whom correspondence should be addressed at: Harvard School of Public Health, Department of Nutrition, Bldg. 2, Rm. 245, 665 Huntington Avenue, Boston, MA 02115.

cess at the plasma membrane (7). A 40-kDa plasma membrane fatty acid-binding protein ($FABP_{PM}$) is thought to be involved in long chain FFA uptake, and has been isolated from jejunum as well as liver and adipose cells (7–9). In the intestine, $FABP_{PM}$ has been localized primarily to the apical membrane of the enterocytes, with lesser amounts on the basolateral membrane (8).

In order to study the polarity of FFA uptake and metabolism in the intestinal cell, a system whereby one can separately manipulate the medium on the apical and basolateral sides of the epithelium is required. Cultures of intact sheets of normal intestinal epithelium are impractical because the normal basolateral membrane organization is rapidly lost (10). Caco-2 is a human colon adenocarcinoma cell line that has been shown to be a useful in vitro model for small intestinal epithelium. When grown on plastic or permeable filters, Caco-2 differentiates into an enterocyte-like cell with microvillus and basolateral membranes separated by tight junctions (11, 12). Culture on permeable filters allows separate access to the apical and basolateral surfaces of the cells. Differentiated Caco-2 cells express the intestine-specific enzymes sucrase and alkaline phosphatase, and the activities reach approximately half the activities in small intestine (13). Field, Albright, and Mathur (14) report that rates of lipid synthesis in Caco-2 cells are similar to those of isolated rat enterocytes under comparable culture conditions. Further, Caco-2 cells synthesize and secrete apoB-containing lipoproteins (15) in a polarized manner (16), and lipoprotein formation appears to be regulated by the presence of FFA (17–20).

In the present studies, we used the Caco-2 cell line to study directly the polarity of long chain FFA uptake and metabolism in the enterocyte. We have compared the uptake of palmitic acid, a major dietary fatty acid, added to the apical versus the basolateral sides of filter-grown Caco-2 monolayers. In addition, the intracellular metabolism of apically versus basolaterally added palmitate was determined. The results show that the net uptake of palmitate is significantly greater at the apical plasma membrane. In addition, a modest increase in the incorporation of FFA into TG relative to PL for apically, as compared to basolaterally, administered FFA was observed.

MATERIALS AND METHODS

Cell culture

Caco-2 cells were obtained at passage 19 from the American Type Culture Collection (Rockville, MD), and cells from passages 20 through 42 were used for all experiments. Cells were cultured in Dulbecco's Modified Eagle's Medium (DMEM) with 4.5 g/l glucose, 4 mM glutamine, 100 U/ml penicillin, and 100 μg/ml streptomycin (Gibco-BRL, Grand Island, NY) and supplemented with 15% fetal bovine serum (FBS, Hyclone, Logan, UT) and 1% nonessential amino acids (Gibco-BRL) in a 95% air/5% CO_2 atmosphere at 37°C. Cells were maintained in 175-cm^2 flasks (Falcon, Lincoln Park, NJ). They were plated at densities $\geq 10^4/cm^2$ and were split when they reached 70–90% confluence using 0.25% trypsin–1 mM EDTA (Gibco-BRL). In all cases the medium was changed at least three times per week.

For the experiments, cells were plated at a density of $4 \times 10^5/cm^2$ (near confluent density) on 6-mm or 24-mm polycarbonate Transwell filter inserts with 0.4 μm pores (Costar, Cambridge, MA). The inserts fit into 24-well or 6-well culture plates, respectively, thereby allowing separate access to the upper and lower surfaces of the cell monolayers. Tight junction formation was assessed in two ways. The flux of the impermeant fluorophore Lucifer Yellow (0.5 mM; Sigma, St. Louis, MO) across the monolayer (apical to basolateral) was measured at 37°C (12) in order to determine the extent of paracellular diffusion of a marker with a molecular weight (mol wt 457) similar to long chain FFA. Transepithelial resistance was monitored with a Millicell-ERS apparatus (Millipore, Bedford, MA). Alkaline phosphatase activity was determined by the method of Ray (21) as modified by Hubbard, Wall, and Ma (22), and sucrase was determined as described by Dahlqvist (23).

Electron microscopy

Cells were plated and grown on filters as for experiments. Monolayers were fixed in 2.5% glutaraldehyde buffered with 0.1 M sodium cacodylate for 1 h at 4°C. The cells were then post-fixed for 30 min in 1% osmium tetroxide in sodium cacodylate buffer. After post-fixation, the cells were stained *en bloc* with uranyl acetate, dehydrated with graded ethanols and propylene oxide, and embedded in Epox 812 resin (24). Ultrathin sections were cut on an MT 6000 microtome, stained with uranyl acetate and lead citrate, and examined with a Philips 300 electron microscope.

Fatty acid uptake studies

Solutions of 200 μM [^{3}H]palmitate (New England Nuclear, Boston, MA) complexed to 50 μM bovine serum albumin (BSA, essentially fatty acid-free; Sigma, St. Louis, MO) were made by addition of [^{3}H]palmitate from ethanolic stock (<0.5% v/v) to BSA in phosphate-buffered saline (137 mM NaCl, 2.7 mM KCl, 1.5 mM KH_2PO_4, 8 mM Na_2HPO_4, pH 7.4) supplemented with 25 mM glucose, 10 μM $CaCl_2$ and 1 mM $MgCl_2$ (PBS-GCM) to make a solution with specific activity of 500–1200 dpm/pmol.

Caco-2 monolayers were grown on filters for 6 to 9 days and used only when the transepithelial resistance was ≥ 200 ohm · cm^2. Monolayers were cultured overnight in serum-free medium or, as noted, in serum-free medium

plus 50 μM BSA to which 50 μM palmitate (Nu-Chek Prep, Elysian, MN) was added from ethanolic stock (<0.5% v/v, with equal ethanol in control medium without palmitate). Monolayers were washed twice with PBS-GCM at 37°C, and the ^{3}H-labeled FFA solution was then added to the upper (apical, 200 μl) or lower (basolateral, 400 μl) compartment of the Transwell insert. PBS-GCM was added to the opposite side of the monolayer. The cells were incubated at 37°C for 2–120 min. Uptake was stopped by removing the incubation medium and washing the monolayers twice on ice for 5 min with 1% BSA in PBS-GCM. In separate experiments, it was found that washing cells on ice with BSA at concentrations above 0.5% for at least 5 min saturably removed extracellular FFA (data not shown). The monolayers were then washed three times with PBS, scraped into 1 ml PBS with a rubber policeman, and sonicated for 30 sec. Aliquots were removed and solubilized in Ultrafluor (National Diagnostics, Manville, NJ), and radioactivity was quantified using a Beckman LS-5000TD liquid scintillation counter (48% efficiency for ^{3}H). FFA uptake was determined from the specific activity of the incubation medium. Protein was determined by the method of Lowry et al. (25). Unbound concentrations of palmitate were determined using the palmitate association constants for BSA reported by Spector, Fletcher, and Ashbrook (26), and a calculation program kindly provided by Drs. Luis Isola and Paul Berk (Mt. Sinai Medical Center, NY), and based on the method of Wosilait and Nagy (27).

Surface area determination

Relative apical and basolateral membrane surface areas of Caco-2 cells were determined by partitioning of the impermeant fluorophore 1-[4-(trimethylamino)phenyl]-6-phenylhexatriene (TMA-DPH; Molecular Probes, Eugene, OR) between the cells and unsealed erythrocyte ghosts, using a modification of the technique described by Lange et al. (28). This method assumes equal partitioning of the TMA-DPH between ghost membranes and cell plasma membranes. TMA-DPH labels only the plasma membrane of intact cells and appears to remain in the outer leaflet of the membrane bilayer (29). Moreover, since tight junctions are a diffusion barrier between the outer leaflets of the apical and basolateral membranes (30), partition of TMA-DPH between unsealed ghosts and cells could be used to assess the relative apical and basolateral surface areas of Caco-2 cells. The surface area of an unsealed ghost was taken as 297 μm^2, 2.2-times greater than the reported surface area of 135 μm^2 for sealed ghosts (28, 31). Apical surface area of Caco-2 cells was determined using tight monolayers (>300 ohm · cm^2), and total surface area using monolayers that were made leaky (~70 ohm · cm^2) by incubation with 1 mM EDTA in PBS (pH 8) for 10 min at room temperature. Basolateral surface area was calculated by subtracting the apical from the total surface area.

Caco-2 monolayers (approximately 2 × 10^6 cells) on 24-mm filters were incubated with gentle shaking for 5 min at room temperature with 10^6/ml unsealed erythrocyte ghosts prepared as described by Steck (32), and labeled with 1 μM TMA-DPH. Incubations were in PBS (pH 8.0). Two ml ghosts plus TMA-DPH were added to the apical compartment and 3 ml PBS to the basolateral. After the incubation, the ghost suspension was removed and saved, the Caco-2 monolayer was rinsed, and the rinse was added to the ghosts. Cell debris was removed from ghosts by spinning at 400 *g* for 10 min at 4°C. The ghosts were then pelleted at 23,000 *g* for 15 min at 4°C and resuspended in 0.5 or 1 ml PBS. Caco-2 cells were scraped into the same volume of PBS and sonicated for 30 sec. The number of Caco-2 cells recovered was estimated by average protein per cell (0.73 ± 0.04 ng/cell, n = 3). Aliquots of ghosts and cells were solubilized in 0.5 or 1% Triton X-100 (National Diagnostics, Highland Park, NJ), and TMA-DPH fluorescence was measured using an SLM 8000 spectrofluorimeter, with excitation at 360 nm and emission at 430 nm. TMA-DPH concentration was quantified by using standard curves of probe added to Triton X-100 mixed with ghosts or cell sonicates.

Fatty acid metabolism studies

Submicellar solutions of [^{3}H]palmitate were made by addition from ethanolic stock (<0.5% v/v) to PBS-GCM, and palmitate concentration (0.6 ± 0.1 μM) was determined relative to the specific activity (35,000 dpm/pmol) of the stock. Monolayers were incubated at 37°C with the submicellar palmitate solution apically (200 μl) or basolaterally (400 μl), and washed as described above. Total cell lipid was extracted using the method of Bligh and

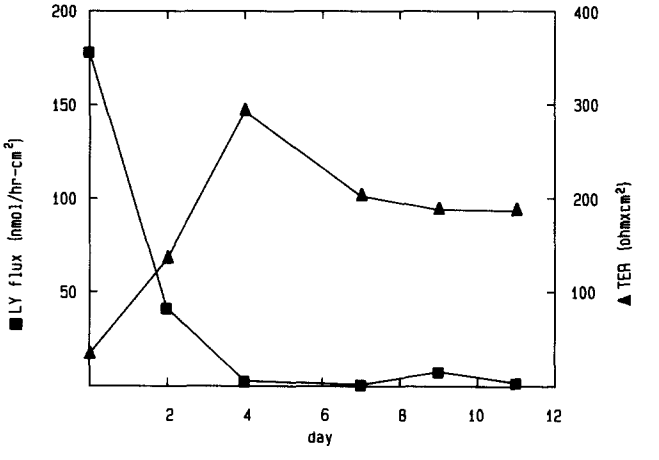

Fig. 1. Development of tight monolayers of filter-grown Caco-2 cells. Transepithelial resistance (TER, ▲) and Lucifer Yellow flux (LY flux, ■) were monitored during differentiation as described in Methods. Data points represent the average of two filters.

Dyer (33), and extraction was found to be approximately 80% efficient based on the recovery of radioactive lipid added to the cell sonicate. After accounting for extraction efficiency, FFA oxidation was estimated by subtraction of the radioactivity recovered in the lipid extract from that in the cell sonicate, and averaged less than 2%. [^{3}H]Palmitate incorporation into lipid metabolites was determined using two-step TLC as described previously (34). Extracts with added carrier lipids (authentic cholesteryl oleate (CE), triolein (TG), oleate (FFA), diolein (DG), and monoolein (MG) from Nu-Chek Prep, and phosphatidic acid (PA), phosphatidylcholine (PC), phosphatidylethanolamine (PE), and phosphatidylserine (PS) from Avanti Polar Lipids, Birmingham, AL) were spotted under nitrogen gas onto 20 × 20 cm flexible TLC plates (polyester-backed silica gel G; Whatman, Hillsboro, OR). The TLC plates were activated before spotting by development in chloroform–methanol 2:1 and drying in a 100°C oven for 60 min. The plates were developed to half the height of the plate in chloroform–methanol–acetic acid–formic acid–water 35:15:6:2:1, allowed to dry, and then developed up the entire height of the plate in hexane–diethyl ether–acetic acid 70:30:1. (Solvents are given in volume ratios.) Lipids were visualized with iodine vapor. After allowing the iodine to evaporate, the area corresponding to each lipid was cut out, placed in 10 ml Ultrafluor, and counted. The metabolism of [^{3}H]palmitate was determined by the percent of radioactivity found in each lipid fraction. Less than 5% of the counts were unidentified, and these were not included in calculations. Where metabolism is expressed as a ratio of TG to phospholipid (PL), PL includes PC, PE, and PS.

Electrophoresis and immunoblotting

Western analysis was used to detect a protein in Caco-2 cytosol that was immunoreactive with antibody to cytosolic rat liver fatty acid-binding protein (L-FABP). The rabbit polyclonal antibody was generously provided by Dr. Teruo Ono (Niigata University School of Medicine, Niigata, Japan). Comparable results were obtained using an antibody generously provided by Dr. Nathan Bass, University of California, San Francisco. Cross-reactivity with human L-FABP in Caco-2 cells was anticipated inasmuch as the proteins are 82% homologous (35). Proteins were separated by sodium dodecyl sulfate polyacrylamide gel electrophoresis (SDS-PAGE) using 15% gels (36). The separated proteins were electrophoretically transferred to PVDF membrane (Immobilon-P; Millipore) according to the method of Matsudaira (37). The blotting membrane was blocked with 5% nonfat dry milk

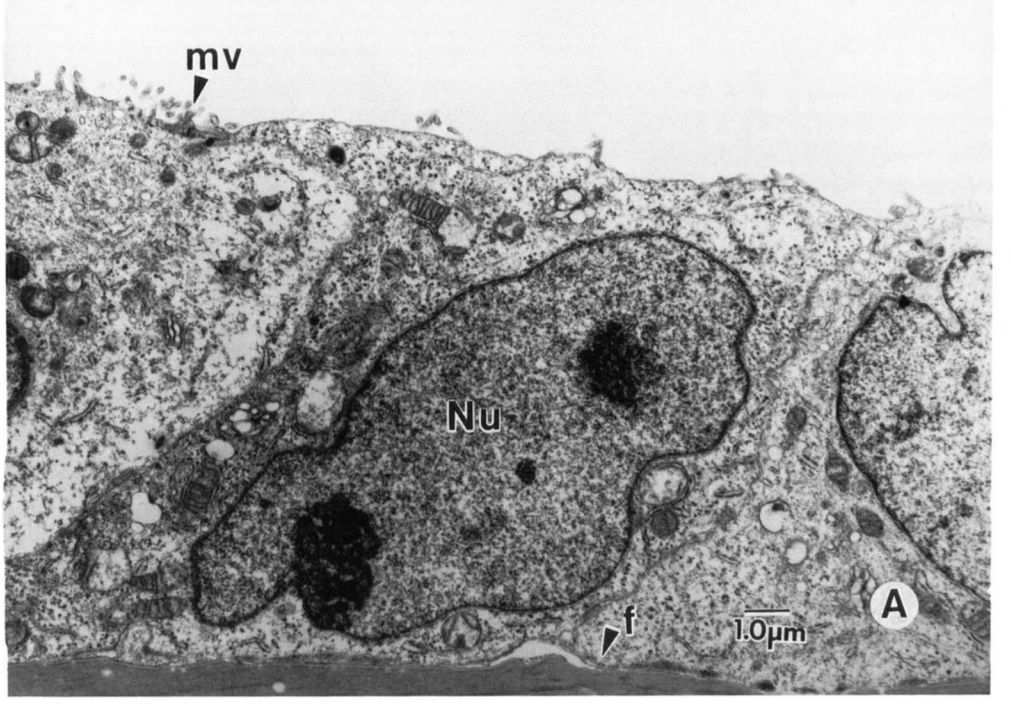

Fig. 2. Electron micrographs of Caco-2 cells grown on filters (f). Cells were plated as for experiments, and fixed for microscopy on day 2 (A) and day 7 (B). Note that at day 2 (A) cells are relatively flat and have few unorganized microvilli (MV). Day 7 cells (B) are columnar and (inset) have tight junctions (TJ) and prominent microvilli (MV); magnification: A, 5,980 ×; B, 4,400 ×; inset, 16,800 ×.

and then incubated with the anti-L-FABP antibody at a 1:100 dilution. Antigen–antibody complexes were detected by incubating the membrane with goat anti-rabbit IgG-horseradish peroxidase conjugate (1:3000; Pierce, Rockford, IL), and finally with 4-chlor-1-naphthol (0.3 mg/ml) and H_2O_2 (0.03%). Corresponding blots incubated with normal rabbit serum showed no reactivity.

Statistical analysis

Data are expressed as the mean ± standard error. *P* values were calculated by Student's *t*-test or paired *t*-test as noted.

RESULTS

Caco-2 cells plated on permeable polycarbonate filters differentiate into polarized epithelial cells with characteristics of small intestine. The levels of enterocyte-specific enzymes increase during differentiation. At 8 days after plating, the cells express sucrase (1.52 ± 0.05 mU/mg, n = 4) and alkaline phosphatase (10.7 ± 0.9 mU/mg, n = 4); these activities are similar to those reported by others for Caco-2 (14). In addition, development of tight junctions between Caco-2 cells grown on filters was evidenced by the decrease in transepithelial flux of the im-

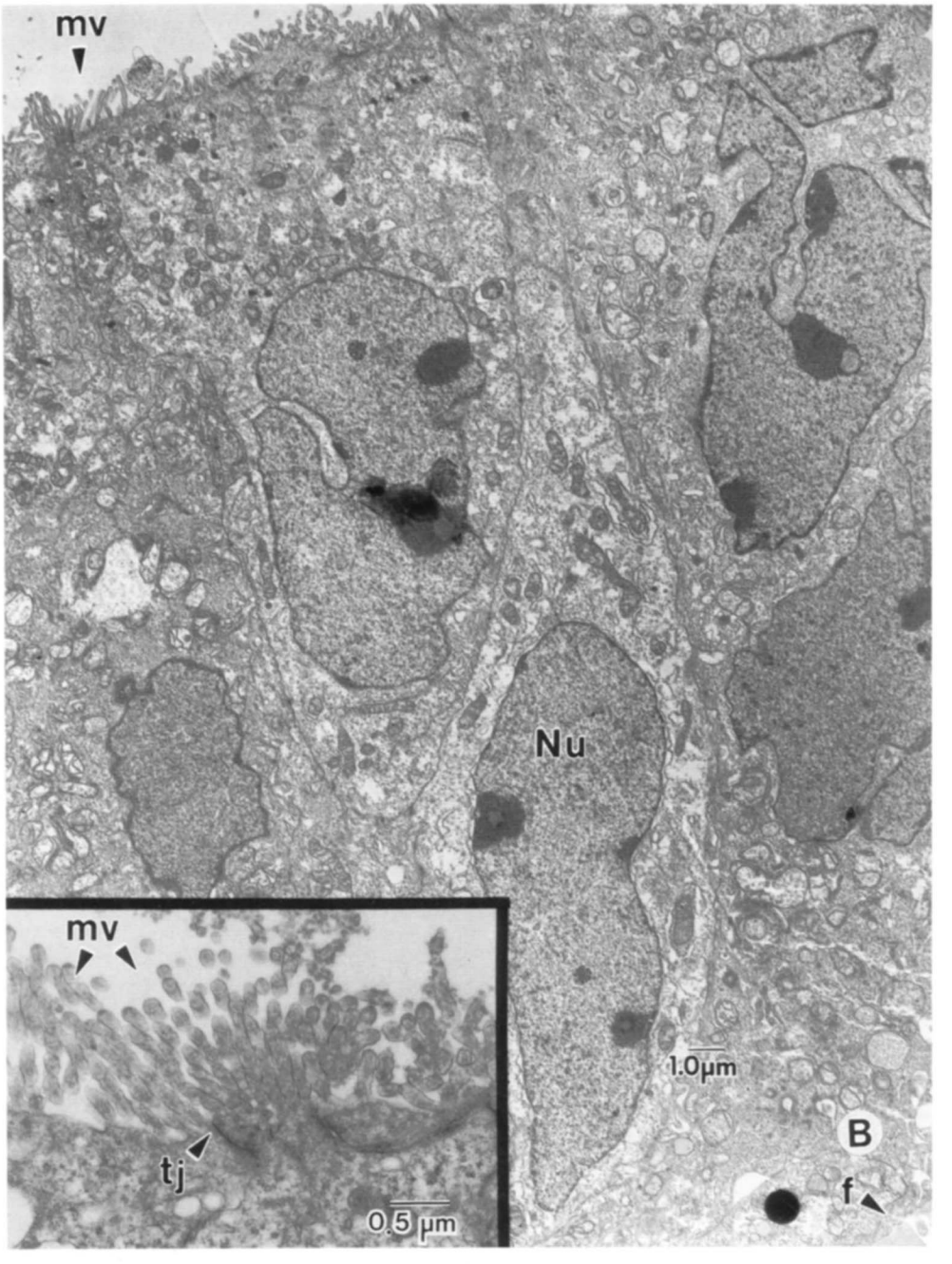

permeant fluorophore Lucifer Yellow, and by the concomitant increase in transepithelial resistance (**Fig. 1**). Electron microscopy revealed that Caco-2 cells had ultrastructural characteristics consistent with those of small intestine. After 2 days, cells attached to the filter and began to form intercellular contacts, but were relatively flat and had only a few short unorganized microvilli (**Fig. 2A**). By day 7, the cells had become tall and columnar, and had developed junctional complexes and many taller microvilli (Fig. 2B and inset).

The total uptake of [^{3}H]palmitate from apical and basolateral solutions of BSA:palmitate (1:4, mol:mol) is shown in **Fig. 3.** The net uptake from both apical and basolateral compartments appears linear with time, but the net accumulation of apical FFA is approximately twice that of basolateral accumulation at all time points measured. The absolute amount of apical and basolateral uptake was independent of the volume of incubation medium placed in the apical and basolateral compartments (data not shown). Experiments using submicellar palmitate concentrations (no BSA) showed approximately equal levels of uptake from apical and basolateral compartments, and absolute levels of uptake that were lower than from BSA-bound FFA despite similar calculated unbound concentrations. However, these studies were complicated by the fact that in the absence of BSA, FFA sticks to the filter and culture well, making quantitation of basolateral accumulation, in particular, very difficult.

To determine whether the greater apical uptake was due to greater apical plasma membrane surface area, or whether the observed differences were independent of the absolute area available for transport, the relative apical and basolateral membrane surface areas were determined. Relative partition of the impermeant fluorophore TMA-DPH between erythrocyte ghosts and intact or EDTA-treated Caco-2 monolayers was used to quantify the surface area of apical and basolateral plasma membranes, as described in Methods. Results show that the ratio of apical:basolateral membrane surface area is approximately 1:3. The apical surface area is 4,123 ± 391 μm^2 and the basolateral area is 12,414 ± 1,055 μm^2 (n = 7). Thus, when the net FFA uptake is normalized for relative surface area, it appears that apical uptake of palmitate is about sixfold greater than basolateral uptake.

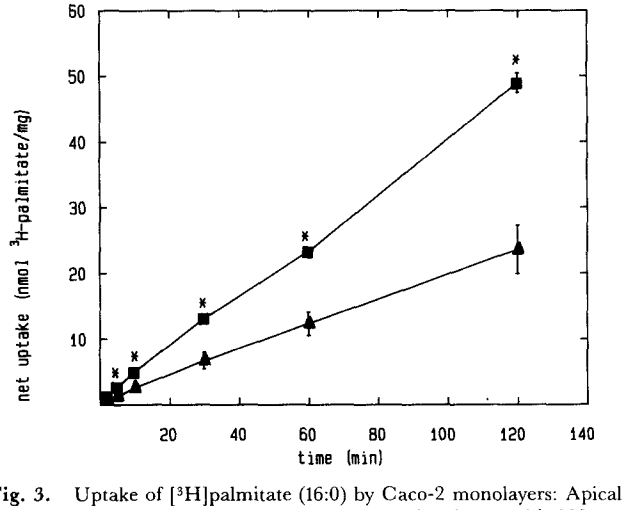

Fig. 3. Uptake of [^{3}H]palmitate (16:0) by Caco-2 monolayers: Apical (AP) versus basolateral (BL). Monolayers were incubated with 200 μM [^{3}H]palmitate complexed to 50 μM BSA in either the AP (■) or BL (▲) compartment for various periods of time. The data represent the mean ± SE for three filters; *, $P < 0.05$ or lower for AP compared to BL.

Caco-2 monolayers were incubated with submicellar concentrations of [^{3}H]palmitate (0.6 μM), and the relative metabolic fate of apically and basolaterally administered FFA was determined (**Table 1**). Results are expressed as percent incorporation into each lipid class. Both apically and basolaterally added palmitate are primarily esterified to TG and PC. The substantial amount of palmitate incorporation into PC as well as TG is consistent with esterification via the glycerol-3-phosphate pathway (38). Relative TG accumulation increased up to 60 min, whereas incorporation into other metabolites remained at a relatively constant level (PL, CE) or decreased (DG, PA) with time. A small but significant difference in metabolic fate of apically versus basolaterally added FFA was evident. Palmitate added at the apical surface was incorporated somewhat more into TG than was basolateral palmitate (**Fig. 4A**), and basolateral palmitate was incorporated more into PL than apical palmitate (Fig. 4B). These differences increased with time of incubation up to 60 min. Although the differences in TG and PL metabolism are small, the polarity of FFA metabolic fate is more apparent when the data are expressed as the TG:PL ratio for each monolayer (Fig. 4C). The TG:PL ratio was 4% higher for apical FFA than for basolateral FFA at 2 min, and the difference rose to 20% by 60 min ($P < 0.025$, paired t-test). By 120 min the increase in percent TG leveled off (Fig. 4A) and the difference in apical and basolateral metabolism decreased, perhaps owing to TG secretion via lipoproteins (19). Addition of 2-monoolein (MG) to the submicellar palmitate solution (molar ratio 2:1, palmitate:MG) did not significantly alter the metabolic fate of palmitate at 10 min (data not shown).

Since it is possible that metabolism is affected by substrate availability, the effect of palmitate preincubation on [^{3}H]palmitate incorporation was examined and the results are shown in **Table 2.** Monolayers were incubated for 18 h with serum-free medium with or without palmitate (50 μM) complexed to albumin (50 μM) in both the apical and basolateral compartments, and were then washed and incubated with [^{3}H]palmitate (0.6 μM) for 10 min, as described above. FFA preincubation caused a significant increase in the incorporation of palmitate into TG relative to PL for both apically and basolaterally administered FFA (Table 2, Set A). Net uptake was not affected

TABLE 1. Incorporation of [^{3}H]palmitate by Caco-2 monolayers

Lipid Class	Percentage of Total Incorporation[a]					
	Apical			Basolateral		
	2 Min	15 Min	60 Min	2 Min	15 Min	60 Min
CE	2.0 ± 0.1	2.4 ± 0.5	2.2 ± 0.2	1.5 ± 0.1	1.4 ± 0.2	1.6 ± 0.3
TG	34.2 ± 1.3	45.9 ± 1.4[b]	58.0 ± 1.2[b]	32.2 ± 0.7	40.7 ± 1.1	54.0 ± 0.7
DG	12.3 ± 0.8	6.3 ± 0.8	4.6 ± 0.6	10.6 ± 0.8	8.3 ± 0.6	4.7 ± 0.9
MG	8.3 ± 0.5	4.9 ± 0.4	3.7 ± 0.4	8.1 ± 0.5	6.1 ± 0.6	4.5 ± 0.5
PA	10.7 ± 0.8	4.2 ± 0.5	2.7 ± 0.4	12.5 ± 0.9	4.6 ± 0.5	2.3 ± 0.3
PE + PS	5.0 ± 0.5	4.2 ± 0.8	6.0 ± 0.5	5.6 ± 0.5	10.0 ± 0.9	6.3 ± 0.4
PC	27.6 ± 0.6	28.8 ± 1.0	22.8 ± 0.5[b]	29.8 ± 0.8	28.9 ± 1.8	26.6 ± 1.0

[a]Mean % of total radioactive palmitate incorporated into metabolite (not including FFA) ± SEM; n = 10 at 2 min, n = 6 at 15 min, and n = 5 at 60 min. The percent FFA at 2, 15, and 60 min for apical was 9.6, 8.5, and 6.6%, and for basolateral was 18.1, 12.8, and 7.1%, respectively. (Differences between apical and basolateral incorporation were also statistically significant when FFA were included in the calculations.)

[b]$P < 0.05$ or lower as compared to basolateral by paired t-test.

(data not shown). Addition of monoolein (100 μM) to the preincubation medium containing palmitate complexed to BSA increased further the incorporation of [^{3}H]palmitate into TG over PL (Table 2, Set B), again without affecting net palmitate uptake (data not shown). Preincubation with FFA or FFA plus MG abolished the apical-basolateral polarity of FFA metabolism observed when cells were preincubated in the absence of lipid.

Two separate cytosolic fatty acid-binding proteins (FABP) are expressed in small intestinal epithelium, the intestinal (I-FABP) and liver (L-FABP) forms (39). These proteins are thought to be involved in FFA uptake and metabolism (40). Caco-2 is reported to lack I-FABP mRNA expression (41). In order to establish the presence of L-FABP in Caco-2, Western analysis was performed. **Fig. 5** shows that Caco-2 cells express L-FABP, and that L-FABP abundance increases by about twofold during differentiation. The apparent level of reactive protein was lower in Caco-2 than in rat intestinal cytosol. This might be due to lower reactivity of the anti-rat L-FABP antibody with human L-FABP. However, Coomassie blue-stained SDS-PAGE gels showed that the protein band corresponding to FABP was much lighter in Caco-2 than in rat intestine cytosol, perhaps due to the lack of I-FABP as well as lower L-FABP levels (data not shown).

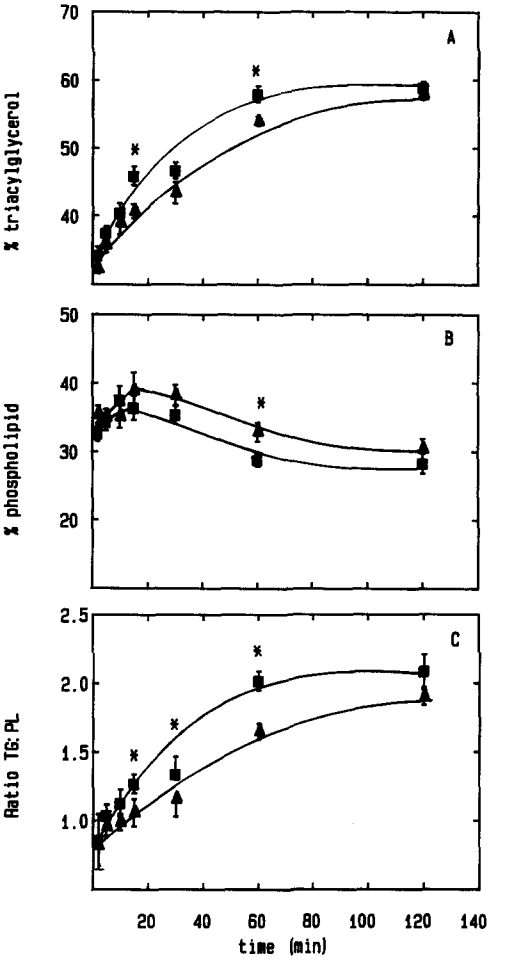

Fig. 4. Metabolism of [^{3}H]palmitate (16:0) by Caco-2 monolayers: Apical (AP, ■) versus basolateral (BL, ▲). Sonicates of cells incubated with 0.6 μM 16:0 were analyzed as described in the text. (A) Percent 16:0 esterified to triacylglycerol (TG). (B) Percent 16:0 incorporated into phospholipid (PL), including phosphatidylcholine, phosphatidylethanolamine, and phosphatidylserine. (C) Ratio of 16:0 esterified to TG as compared to PL. Data are expressed as the mean ± SE for 5 to 11 filters; *, $P < 0.05$ or lower for AP compared to BL by paired t-test.

DISCUSSION

The Caco-2 cell line has been used to examine the polarity of intestinal cell protein and membrane transport (42, 43) as well as to study intestinal lipoprotein metabolism (15–17, 19, 20). Caco-2 cells express sucrase and alkaline phosphatase activities that are characteristic of small intestine enterocytes. Cells plated on filters have a morphology similar to differentiated enterocytes (Fig. 2). Intercellular tight junction formation is evidenced by the

TABLE 2. Effect of palmitate and palmitate-monoolein preincubation (18 h) on palmitate incorporation (10 min) by Caco-2 monolayers

Treatment[a]	Apical		Basolateral	
	% TG[b]	TG:PL[c]	% TG	TG:PL
Set A				
(−) FFA	39.1 ± 0.7	0.98 ± 0.02	36.3 ± 0.3	0.94 ± 0.02
(+) FFA	44.0 ± 1.1	1.37 ± 0.09	44.7 ± 0.8	1.45 ± 0.07
	$P < 0.025$[d]		$P < 0.005$	
Set B				
(+) FFA	42.2 ± 0.6	1.36 ± 0.06	36.9 ± 0.5	1.35 ± 0.05
(+) FFA, MG	47.5 ± 0.3	1.73 ± 0.03	51.1 ± 0.5	2.27 ± 0.09
	$P < 0.05$		$P < 0.025$	

[a]Monolayers were grown for 18 h in serum-free medium ± 50 μM palmitate complexed to 50 μM BSA (Set A), or with 50 μM palmitate complexed to 50 μM BSA ± 100 μM 2-monoolein (Set B). Additions were to both the apical and basolateral compartments. Incubation was carried out for 10 min.

[b]Mean % of total [^{3}H]palmitate (not including free palmitate) incorporated into TG ± SEM; n = 6 for Set A and n = 3 for Set B.

[c]Ratio of [^{3}H]palmitate incorporation into TG to that in PC + PE + PS. Calculated for each sample separately and expressed as mean ± SEM (n = 6 for Set A, n = 3 for Set B).

[d]*P* values were determined by Student's *t*-test.

junctional complexes seen in the electron micrographs, the increasing transepithelial resistance, and the decreasing Lucifer Yellow flux across the monolayer (Fig. 1). Caco-2 cells have been shown to secrete lipoproteins in a polarized manner (16). Therefore, this cell line is well suited to investigate the polarity of FFA uptake and metabolism in the enterocyte.

The net uptake of palmitate (palmitate–BSA 4:1, unbound palmitate concentration 1.3 μM) from the apical compartment was twofold higher than uptake from the basolateral compartment (Fig. 3). As will be discussed below, the relative apical:basolateral plasma membrane surface area was found to be 1:3; thus, the net uptake of palmitate was sixfold greater from the apical compared to the basolateral compartment per unit surface area.

It is possible that the greater apical FFA uptake is due in part to the presence of the 40 kDa $FABP_{PM}$. This protein, which has been found in small intestine and has been proposed to be involved in FFA uptake (7–9), has been shown by immunocytochemical studies of rat intestine to be localized mainly in the apical membrane of the rat enterocyte, with lesser staining of the basolateral membrane (8). The K_m of the $FABP_{PM}$ in jejunal mucosal cells is reported to be 93 nM for oleic acid (9). Consistent with the proposed protein-mediated uptake, our uptake studies for palmitate complexed to BSA showed apparent saturation of net uptake, both at the apical and basolateral surface, for unbound FFA concentrations above 300 nM (data not shown). Furthermore, little increase in net uptake was observed for submicellar solutions of free palmitate ranging from 370 nM to 740 nM (data not shown).

Greater apical FFA uptake might also be related to differences in the plasma membrane composition between the apical and basolateral domains of the cell (44). Alternatively, greater apical uptake could reflect more rapid metabolism of apically absorbed FFA due to greater compartmentalization of enzymes in the apical half of the cell. It is unlikely that the presence of the filter is responsible for the lower basolateral uptake of such a small molecule as palmitate, since the filter pore size is 0.4 μm, and Caco-2 cells secrete lipoproteins through filters with a similar pore size (16). In addition, Shasby, Stoll, and Spector (45) reported apical and basolateral uptake of various FFA by bovine aortic endothelium grown on polycarbonate filters, and found that in some cases FFA uptake was equal or greater at the basolateral surface. Finally, our data show that the increased apical uptake of FFA

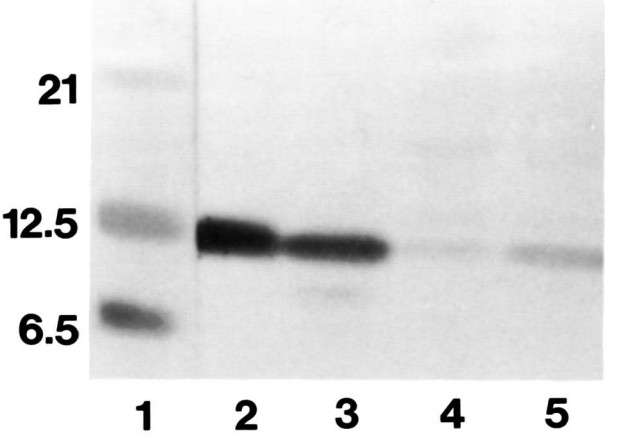

Fig. 5. Immunoblot of L-FABP in Caco-2 cells. Proteins were separated by SDS-PAGE, electrophoretically blotted to PVDF membrane, and reacted with anti-LFABP antibody as described in Methods. Lane 1, molecular weight standards (kDa) stained with Coomassie blue; lane 2, 0.3 μg purified rat liver FABP; lane 3, 10 μg rat intestinal cytosolic protein; lane 4, 50 μg cytosolic protein from undifferentiated Caco-2 cells; lane 5, 50 μg cytosolic protein from differentiated Caco-2 cells.

is not due to greater apical plasma membrane surface area. Thus the increased apical uptake is likely to reflect enterocyte-specific FFA transport.

Partitioning of the impermeant cationic fluorophore TMA-DPH (28) between erythrocyte ghosts and Caco-2 cells was used to determine the relative surface areas of apical and basolateral plasma membranes and the results indicate that the ratio of apical to basolateral surface area is approximately 1:3. Morphometric analysis of hamster and rat enterocytes in vivo showed a ratio of 1:1 (46) and 1:1.3 (47), respectively. When rats were treated with colchicine a 1:2.6 ratio was found, and the difference was primarily due to a decrease in the length of the microvilli (47). Measurement of the dimensions of Caco-2 cells showed that the length of the microvilli does not reach that of rat enterocytes (12); therefore, a ratio of 1:3 for apical to basolateral membrane surface seems reasonable for Caco-2 cells.

The absolute surface areas obtained for Caco-2 cells using this partitioning method are about three times larger than enterocyte surface areas obtained using morphometric techniques (46, 47). It is not likely that Caco-2 cells are substantially larger than enterocytes, as the reported total cell height and width (12) are similar. Surface area might be overestimated if TMA-DPH is internalized via transmembrane flip-flop or endocytosis. However, Storch, Shulman, and Kleinfeld (29) found no evidence of TMA-DPH internalization in 3T3F442A cells for at least 10 min at room temperature. Thus, the TMA-DPH fluorescence likely arises from partitioning into the plasma membrane only. It is noteworthy that the plasma membrane surface areas obtained using TMA-DPH, as originally reported by Lange et al. (28), are much larger than the surface areas reported for similar cells using stereologic techniques. For example, the absolute surface area of canine liver cells, as determined with TMA-DPH, was sevenfold larger than that obtained by stereologic determinations for rat liver cells (48). It is conceivable that the TMA-DPH method, which is based on the partitioning of a fluorophore into the membrane, might measure fine structure of the membrane that is not detected by morphometry.

The present results with the Caco-2 cell line show that a somewhat greater percentage of apical as compared to basolateral FFA is incorporated into TG. In addition, incorporation into PL is increased to a small extent for basolateral as compared to apical FFA (Fig. 4). Thus, the TG:PL ratio is 20% greater for apical FFA at 60 min, although this degree of metabolic polarity is far less than that reported in vivo. The in vivo studies (3, 4) showed that FFA taken up from the lumen of the intestine are esterified primarily to TG (60%), whereas plasma FFA are oxidized (42%) and incorporated into PL (28%). Interestingly, a similar polarity of FFA metabolism was found in the crypt as well as the villus cells (3). It was suggested that the marked polarity of FFA utilization was a result of the structural or functional polarity of the enterocyte. For instance, ultrastructural studies have demonstrated a more apical localization of endoplasmic reticulum (ER) and Golgi (49), and of the monoacylglycerol and glycerol-3-phosphate acyltransferases present in the smooth and rough ER, respectively (50). On the other hand, mitochondria were found to be uniformly distributed in the cell (49). Thus, the small differences between apical and basolateral FFA metabolism observed in Caco-2 cells may reflect a polarity of enzyme activity or pools of intermediary metabolites.

The percentage incorporation of FFA into TG by Caco-2 is lower than that reported for lumenal FFA, but higher than that for plasma FFA (3). Preliminary results suggest that Caco-2 cells may have a lower total acytransferase capacity than do mature intestinal cells (data not shown). The in vivo studies (3, 4) also showed significant oxidation of plasma FFA (42%) and little oxidation (15%) of lumenal FFA. In contrast, virtually no oxidation ($<2\%$) of either apical or basolateral FFA was observed in Caco-2 cells. The cells were grown in high glucose medium (25 mM), so that glucose was in excess under the experimental conditions used. A recent report shows that Caco-2 cells synthesize and store glycogen (51). Thus, it is not surprising that glucose might be preferentially utilized as a source of fuel (52). Increased FFA oxidation might be expected using lower glucose concentrations. Experiments in which filter-grown Caco-2 monolayers were preincubated in the absence of glucose were not possible, however, because the transepithelial resistance was lost in monolayers preincubated without glucose.

The lack of marked polarity of FFA metabolism in Caco-2 cells could be due to a number of factors. Although, as discussed above, Caco-2 cells are a good model of small intestinal epithelium, they express some characteristics consistent with less differentiated crypt cells (11, 53). Nevertheless, polarity of FFA metabolism was described not only in villus cells but also in the relatively less absorptive crypt cells (3). Another possible explanation might be that these cultured cells are not exposed to hormones that affect FFA metabolism in vivo. For example, Vidal et al. (54) have reported that vasoactive intestinal peptide causes a switch from glucose to FFA oxidation in isolated rat enterocytes.

Differences in FABP levels or activities might also be considered as a possible cause of the less marked metabolic polarity. FABP have been suggested to play a role in cellular uptake of FFA, modulation of enzyme activities, and targeting of FFA to specific organelles (40). The small intestinal epithelium expresses both the intestinal (I-FABP) and liver (L-FABP) forms of FABP (39). Caco-2 lacks I-FABP mRNA expression (41) and we were unable to detect it on Western blots using an anti-rat I-FABP antibody (data not shown). Fig. 5 shows that Caco-2 cells do ex-

press L-FABP. Although no consistent differences in subcellular localization of I-FABP and L-FABP in the enterocyte have been found (39, 55), L-FABP and I-FABP differ in characteristics of ligand binding (56) and in regulation of expression (57). It has been proposed that the two FABPs have different functions within the enterocyte, perhaps related to the polarity of FFA metabolism (56). However crypt cells, which as mentioned above were demonstrated to have polarity of FFA metabolism comparable to villus cells (3), have little or no expression of either FABP (39, 55, 58, 59). Thus it seems unlikely that the lack of I-FABP in Caco-2 cells should affect metabolic polarity, but the question requires further study.

Finally, the Caco-2 cells were grown under relatively unpolarized nutritional conditions as compared to enterocytes in situ. Monolayers received the same medium apically and basolaterally throughout differentiation. The enterocytes of the intestine, on the other hand, are periodically exposed to relatively large amounts of dietary lipid at the apical surface and continuously exposed to small amounts of FFA from the plasma, at the basolateral surface. Such extracellular nutritional polarity may contribute to the metabolic polarity within the enterocyte, since it has been reported that lipid-metabolizing enzymes are sensitive to substrate availability (60, 61), and that the subcellular localization of lipid metabolic enzymes may be polarized (50). Our results (Table 2) support the concept that either enzyme activation or increased storage of metabolic intermediates (e.g., diacylglycerol) occurs in Caco-2 when substrate availability is increased. Perhaps the apical compartmentalization of lipid-esterifying enzymes within the enterocyte described by Higgins and Barrnett (50) occurs in response to greater lipid concentration in the lumen of the intestine. Under unpolarized nutritional conditions, such compartmentalization may not occur.

In conclusion, we have used the Caco-2 cell line to study the polarity of FFA uptake and metabolism at the level of the enterocyte. Net apical uptake of palmitate is markedly greater than basolateral uptake. A somewhat greater percentage of apical as compared to basolateral palmitate is incorporated into TG. More pronounced polarity of FFA metabolism may be dependent upon extracellular factors such as hormones and substrate availability.

We thank Dr. Angeline Warner and Ms. Cindy Rosenblad for their generous assistance with the electron microscopy. We also thank Dr. Teruo Ono, at the Niigata University School of Medicine, Japan, and Dr. Nathan Bass, at the University of California San Francisco, for providing anti-liver and anti-intestine FABP antibodies. We also thank Dr. Paul Berk and Dr. Luis Isola, at the Mt. Sinai Medical Center, New York, for the program for calculating unbound FFA concentrations. Dr. Hye-Kyung Kim of our laboratory kindly provided the purified rat L-FABP. In addition, we thank Drs. Steven Furlong, James Madara, and Marian Neutra for helpful discussions. This investigation was supported by National Institutes of Health Grants DK38389 (J. S.) and DK34854 (Harvard Digestive Diseases Center) and a National Science Foundation Graduate Fellowship (P. J. T.).

Manuscript received 3 August 1990 and in revised form 2 October 1990.

REFERENCES

1. Shiau, Y. F. 1981. Mechanisms of fat absorption. *Am. J. Physiol.* **240:** G1-G9.
2. Carey, M. C., D. M. Small, and C. M. Bliss. 1983. Lipid digestion and absorption. *Annu. Rev. Physiol.* **45:** 651-677.
3. Gangl, A., and R. K. Ockner. 1975. Intestinal metabolism of plasma free fatty acids. *J. Clin. Invest.* **55:** 803-813.
4. Gangl, A., and F. Renner. 1978. In vivo metabolism of plasma free fatty acids by intestinal mucosa of man. *Gastroenterology.* **74:** 847-850.
5. Thomson, A. B. R., and J. M. Dietschy. 1981. Intestinal lipid absorption: major extracellular and intracellular events. *In* Physiology of the Gastrointestinal Tract. L. R. Johnson, editor. Raven Press, New York. 1147-1220.
6. Cooper, R. B., N. Noy, and D. Zakim. 1989. Mechanism for binding of fatty acids to hepatocyte plasma membranes. *J. Lipid Res.* **30:** 1719-1726.
7. Potter, B. J., D. Sorrentino, and P. D. Berk. 1989. Mechanisms of cellular uptake of free fatty acids. *Annu. Rev. Nutr.* **9:** 253-270.
8. Stremmel, W., G. Lotz, G. Strohmeyer, and P. D. Berk. 1985. Identification, isolation and partial characterization of a fatty acid binding protein from rat jejunal microvillus membranes. *J. Clin. Invest.* **75:** 1068-1076.
9. Stremmel, W. 1988. Uptake of fatty acids by jejunal mucosal cells is mediated by a fatty acid binding membrane protein. *J. Clin. Invest.* **82:** 2001-2010.
10. Neutra, M., and D. Louvard. 1989. Differentiation of intestinal cells in vitro. *In* Functional Epithelial Cells in Culture. K. S. Matlin and J. D. Valentich, editors. Alan R. Liss, New York. 363-398.
11. Grasset, E., M. Pinto, E. Dussaulx, A. Zweibaum, and J. F. Desjeux. 1984. Epithelial properties of the human colonic carcinoma cell line Caco-2: electrical parameters. *Am. J. Physiol.* **247:** C260-C267.
12. Hildalgo, I. J., T. J. Raub, and R. T. Borchardt. 1989. Characterization of the human colon carcinoma cell line (Caco-2) as a model system for intestinal epithelial permeability. *Gastroenterology.* **96:** 736-749.
13. Pinto, M., S. Robin-Leon, M. D. Appay, M. Kedinger, N. Triadou, E. Dussaulx, B. Lacroix, P. Simon-Assman, K. Haffen, J. Fogh, and A. Zweibaum. 1983. Enterocyte-like differentiation and polarization of the human colon carcinoma cell line Caco-2 in culture. *Biol. Cell.* **47:** 323-330.
14. Field, F. J., E. Albright, and S. N. Mathur. 1987. Regulation of cholesterol esterification by micellar cholesterol in Caco-2 cells. *J. Lipid Res.* **28:** 1057-1066.
15. Hughes, T. E., W. V. Sasak, J. M. Ordovas, T. M. Forte, S. Lamon-Fava, and E. J. Schaefer. 1987. A novel cell line (Caco-2) for the study of intestinal lipoprotein synthesis. *J. Biol. Chem.* **262:** 3762-3767.
16. Traber, M. G., H. J. Kayden, and M. J. Rindler. 1987. Polarized secretion of newly synthesized lipoproteins by the Caco-2 human intestinal cell line. *J. Lipid Res.* **28:** 1350-1363.
17. Moberly, J. B., T. G. Cole, D. H. Alpers, and G. Schonfeld.

1990. Oleic acid stimulation of apolipoprotein B secretion from HepG2 and Caco-2 cells occurs post-transcriptionally. *Biochim. Biophys. Acta.* **1042:** 70–80.
18. Dashti, N., E. A. Smith, and P. Alaupovic. 1990. Increased production of apolipoprotein B and its lipoproteins by oleic acid in Caco-2 cells. *J. Lipid Res.* **31:** 113–123.
19. Field, F. J., E. Albright, and S. N. Mathur. 1988. Regulation of triglyceride-rich lipoprotein secretion by fatty acids in Caco-2 cells. *J. Lipid Res.* **29:** 1427–1437.
20. Hughes, T. E., J. M. Ordovas, and E. J. Schaefer. 1988. Regulation of intestinal apolipoprotein synthesis and secretion by Caco-2 cells. *J. Biol. Chem.* **263:** 3425–3431.
21. Ray, T. K. 1970. A modified method for the isolation of plasma membrane from rat liver. *Biochim. Biophys. Acta.* **196:** 1–9.
22. Hubbard, A. L., D. A. Wall, and A. Ma. 1983. Isolation of rat hepatocyte plasma membranes. I. Presence of three major domains. *J. Cell Biol.* **96:** 217–229.
23. Dahlqvist, A. 1968. Assay of intestinal disaccharidases. *Anal. Biochem.* **22:** 99–107.
24. Warner, A. E., B. E. Barry, and J. D. Brain. 1986. Pulmonary intravascular macrophages in sheep: morphology and function of a novel constituent of the mononuclear phagocyte system. *Lab. Invest.* **55:** 276–288.
25. Lowry, O. H., N. J. Rosebrough, A. L. Farr, and R. J. Randall. 1951. Protein measurement with the Folin phenol reagent. *J. Biol. Chem.* **193:** 265–275.
26. Spector, A. A., J. E. Fletcher, and J. D. Ashbrook. 1971. Analysis of long-chain free fatty acid binding to bovine serum albumin by determination of stepwise equilibrium constants. *Biochemistry.* **10:** 3229–3232.
27. Wosilait, W. D., and P. Nagy. 1976. A method of computing drug distribution in plasma using stepwise association constants: clofibrate acid as an illustrative example. *Comp. Prog. Biomed.* **6:** 142–148.
28. Lange, Y., M. H. Swaisgood, B. V. Ramos, and T. L. Steck. 1989. Plasma membranes contain half the phospholipid and 90% of the cholesterol and sphingomyelin in cultured human fibroblasts. *J. Biol. Chem.* **264:** 3786–3793.
29. Storch, J., S. Shulman, and A. Kleinfeld. 1989. Plasma membrane lipid order and composition during adipocyte differentiation of 3T3F442A cells. Studies in intact cells with 1-[4-(trimethylamino)phenyl]-6-phenylhexatriene. *J. Biol. Chem.* **264:** 10527–10533.
30. Van Meer, G., and K. Simons. 1986. The function of tight junctions in maintaining differences in lipid composition between the apical and basolateral cell surface domains of MDCK cells. *EMBO J.* **5:** 1455–1464.
31. Evans, E., and Y. C. Fung. 1972. Improved measurements of erythrocyte geometry. *Microvasc. Res.* **4:** 335–347.
32. Steck, T. L. 1974. Preparation of impermeable inside-out and right-side-out vesicles from erythrocyte membranes. *In* Methods in Membrane Biology. Vol. II. E. D. Korn, editor. Plenum Press, New York. 245–281.
33. Bligh, E. G., and W. J. Dyer. 1959. A rapid method of total lipid extraction and purification. *Can. J. Biochem. Physiol.* **37:** 911–917.
34. Storch, J., and D. Schachter. 1985. Calcium alters the acyl chain composition and lipid fluidity of rat hepatocyte plasma membranes in vitro. *Biochim. Biophys. Acta.* **812:** 473–484.
35. Gordon, J. I., and J. B. Lowe. 1985. Analyzing the structures, function and evolution of two abundant gastrointestinal fatty acid binding proteins with recombinant DNA and computational techniques. *Chem. Phys. Lipids.* **38:** 137–158.
36. Laemmli, U. K. 1970. Cleavage of structural proteins during the assembly of the head of bacteriophage T4. *Nature.* **227:** 680–685.
37. Matsudaira, P. 1987. Sequence from picomole quantities of proteins electroblotted onto polyvinylidene difluoride membranes. *J. Biol. Chem.* **262:** 10035–10038.
38. Johnston, J. M., F. Paultauf, C. M. Schiller, and L. D. Schultz. 1970. The utilization of the α-glycerophosphate and the monoglyceride pathways for phosphatidylcholine biosynthesis in the intestine. *Biochim. Biophys. Acta.* **218:** 124–133.
39. Shields, H. M., M. L. Bates, N. M. Bass, C. J. Best, D. H. Alpers, and R. K. Ockner. 1986. Light microscopic immunocytochemical localization of hepatic and intestinal types of fatty acid-binding proteins in rat small intestine. *J. Lipid Res.* **27:** 549–557.
40. Spener, F., T. Börchers, and M. Mukherjea. 1989. On the role of fatty acid binding proteins in fatty acid transport and metabolism. *FEBS Lett.* **244:** 1–5.
41. Sweetser, D. A., E. H. Berkenmeier, I. J. Klisak, S. Zollman, R. S. Sparkes, T. Mohandas, A. J. Lusis, and J. I. Gordon. 1987. The human and rodent intestinal fatty acid binding protein genes. *J. Biol. Chem.* **262:** 16060–16071.
42. Matter, K., M. Brauchbar, K. Bucher, and H. P. Hauri. 1990. Sorting of endogenous plasma membrane proteins occurs from two sites in cultured human intestinal epithelial cells (Caco-2). *Cell.* **60:** 429–437.
43. Hughson, E. J., and C. R. Hopkins. 1990. Endocytic pathways in polarized Caco-2 cells: identification of an endosomal compartment accessible from both apical and basolateral surfaces. *J. Cell Biol.* **110:** 337–348.
44. Brasitus, T. A., and D. Schachter. 1980. Lipid dynamics and lipid-protein interactions in the rat enterocyte basolateral and microvillus membranes. *Biochemistry.* **19:** 2763–2769.
45. Shasby, D. M., L. L. Stoll, and A. A. Spector. 1987. Polarity of arachidonic acid metabolism by bovine aortic endothelial cell monolayers. *Am. J. Physiol.* **253:** H1177–H1183.
46. Buschmann, R. J., and D. J. Manke. 1981. Morphometric analysis of membranes and organelles of small intestinal enterocytes. I. Fasted hamster. II. Lipid-fed hamster. *J. Ultrastruct. Res.* **76:** 1–14; 15–26.
47. Buschmann, R. J. 1983. Morphometry of the small intestinal enterocytes of the fasted rat and the effects of colchicine. *Cell Tissue Res.* **231:** 289–299.
48. Weibel, E. R., W. Stäubel, H. R. Gnägi, and F. A. Hess. 1969. Correlated morphometric and biochemical studies on the liver cell. I. Morphometric model, stereologic methods and normal morphometric data from rat liver. *J. Cell Biol.* **42:** 68–91.
49. Trier, J. S., and J. L. Madara. 1981. Functional morphology of the mucosa of the small intestine. *In* Physiology of the Gastrointestinal Tract. L. R. Johnson, editor. Raven Press, New York. 925–961.
50. Higgins, J. A., and R. J. Barrnett. 1971. Fine structural localization of acyltransferases. *J. Cell Biol.* **50:** 102–120.
51. Ellwood, K. C., and M. L. Failla. 1990. Impact of medium glucose and serum on glycogen levels in Caco-2 cells. *FASEB J.* **4:** A1165 (Abstract #5222).
52. Shiau, Y. F., W. B. Long, and J. B. Weiss. 1978. Effect of sugar and monoglyceride on fatty acid esterification. *Am. J. Physiol.* **243:** E236–E242.
53. Quaroni, A. 1986. Crypt cell antigen expression in human colon tumor cell lines: analysis with a panel of monoclonal antibodies to Caco-2 luminal membrane components. *J. Natl. Cancer Inst.* **76:** 571–585.
54. Vidal, H., M. Beylot, B. Comte, F. Vega, and J. P. Riou.

1989. Vasoactive intestinal peptide stimulates long-chain fatty acid oxidation and inhibits acetyl-coenzyme A carboxylase activity in isolated rat enterocytes. *J. Biol. Chem.* **264:** 4901–4906.

55. Iseki, S., M. Hitomi, T. Ono, and H. Kondo. 1989. Immunocytochemical localization of hepatic fatty acid binding protein in rat intestine: effect of fasting. *Anat. Rec.* **223:** 283–291.
56. Cistola, D. P., J. C. Sacchettini, L. J. Banaszak, M. T. Walsh, and J. I. Gordon. 1989. Fatty acid interactions with rat intestinal and liver fatty acid-binding proteins expressed in *Escherichia coli*. *J. Biol. Chem.* **264:** 2700–2710.
57. Bass, N. M., J. A. Manning, R. K. Ockner, J. I. Gordon, S. Seetharam, and D. H. Alpers. 1985. Regulation of the biosynthesis of two distinct fatty acid-binding proteins from rat liver and intestine. *J. Biol. Chem.* **260:** 1432–1436.
58. Ockner, R. K., and J. A. Manning. 1974. Fatty acid-binding protein in small intestine. *J. Clin. Invest.* **54:** 326–338.
59. Iseki, S., and H. Kondo. 1990. Light microscopic localization of hepatic fatty acid binding protein mRNA in jejunal epithelia of rats using in situ hybridization, immunohistochemical and autoradiographic techniques. *J. Histochem. Cytochem.* **38:** 111–115.
60. Shiau, Y. F., J. T. Boyle, C. Umstetter, and O. Koldovsky. 1980. Apical distribution of fatty acid esterification capacity along the villus-crypt unit of rat jejunum. *Gastroenterology.* **79:** 47–53.
61. Singh, A., J. A. Balint, R. H. Edmonds, and J. B. Rodgers. 1972. Adaptive changes of the rat small intestine in response to a high fat diet. *Biochim. Biophys. Acta.* **260:** 708–715.